

Full counting statistics of chaotic cavities from classical action correlations

This article has been downloaded from IOPscience. Please scroll down to see the full text article.

2008 J. Phys. A: Math. Theor. 41 365102

(<http://iopscience.iop.org/1751-8121/41/36/365102>)

View [the table of contents for this issue](#), or go to the [journal homepage](#) for more

Download details:

IP Address: 171.66.16.150

The article was downloaded on 03/06/2010 at 07:09

Please note that [terms and conditions apply](#).

Full counting statistics of chaotic cavities from classical action correlations

G Berkolaiko¹, J M Harrison^{1,2} and M Novaes³

¹ Department of Mathematics, Texas A&M University, College Station, TX 77843-3368, USA

² Department of Mathematics, Baylor University, Waco, TX 76798-7328, USA

³ School of Mathematics, University of Bristol, Bristol BS8 1TW, UK

Received 2 June 2008, in final form 16 July 2008

Published 6 August 2008

Online at stacks.iop.org/JPhysA/41/365102

Abstract

We present a trajectory-based semiclassical calculation of the full counting statistics of quantum transport through chaotic cavities, in the regime of many open channels. Our method to obtain the m th moment of the density of transmission eigenvalues requires two correlated sets of m classical trajectories, therefore generalizing previous works on conductance and shot noise. The semiclassical results agree, for all values of m , with the corresponding predictions from random matrix theory.

PACS numbers: 05.45.Mt, 73.23.-b, 03.65.Nk

1. Introduction

Phase-coherent electron transport through ballistic quantum dots displays a number of universal properties if the corresponding classical dynamics is chaotic [1]. These are well described by random matrix theory (RMT), in which the system's scattering matrix is assumed to be a random element of the appropriate ensemble [2], i.e. to be random unitary or unitary symmetric depending on whether the time-reversal symmetry is absent or present, respectively. RMT is therefore concerned with the average behaviour of a collection of different systems within a given universality class determined solely by the existing symmetry. On the other hand, properties of generic individual chaotic systems are expected to agree with the predictions of this theory provided a local energy average is considered, around a classically small but quantum mechanically large energy window. Rigorously deriving this connection between chaos and universality is one of the main challenges of the semiclassical trajectory-based approach to mesoscopic transport [3–5].

As in the case of spectral statistics of closed chaotic systems [6], the main ingredient from the classical dynamics is the existence of correlations between long trajectories. They organize themselves into families according to their action, and the elements of a family differ among themselves only by their behaviour in small regions (much smaller than their total length)

in which some of them have crossings while others have anticrossings. The correlations induced by the existence of crossings are responsible for the emergence of universal quantum properties. This approach has been successful in reproducing RMT results for the average conductance [4, 7], shot noise [8–10], time delay [11] and other properties [5]. All these calculations have a natural perturbative structure in which $1/N$, the inverse number of open quantum channels, plays the role of a small parameter.

In this work we advance this line of investigations by obtaining, using the semiclassical approximation and classical correlations, the full counting statistics of chaotic cavities: the complete set of moments of the density of transmission eigenvalues. Physically, this encodes information about the statistics of the electric current through the system [12–14], viewed as a random time signal. The first two such moments are related to the average conductance and shot noise. Our result is restricted to leading order in $1/N$, and to this extent we conclude that all linear statistical information contained in the RMT of quantum chaotic transport is also contained in the semiclassical approximation.

In order to help put our results in perspective, let us draw an analogy with closed systems. By far the most popular quantity to be calculated in that case is the spectral form factor, the Fourier transform of the 2-point correlation function. The calculation requires taking into account contributions due to pairs of periodic orbits. By contrast, in the present work we consider two sets of trajectories with m elements each for all values of m . In a closed system this would correspond to obtaining all m -point correlation functions.

2. Counting statistics of chaotic transport

Quantum transport is governed by the transmission matrix t , or equivalently the Hermitian matrix tt^\dagger . This matrix has a set $\{T_1, \dots, T_n\}$ of $n = \min\{N_1, N_2\}$ non-zero transmission eigenvalues, where N_1 and N_2 are the number of open channels in the incoming and outgoing leads, respectively. We consider a chaotic cavity with typical dwell time τ_D , Lyapunov exponent λ_L and linear size L . Together with the Fermi wavelength λ_F , these last two quantities define the Ehrenfest time $\tau_E = \lambda_L^{-1} \log(L/\lambda_F)$, roughly the time it takes for an initially localized wave packet to spread to the size of the system. For times much longer than τ_E one can expect any initial state to become effectively equidistributed.

The regime we are interested in is the semiclassical limit $\lambda_F \ll L$, when there are many open channels, $N_1, N_2 \gg 1$. However, we must approach this limit in such a way that τ_D , which is a classical time scale, satisfies $\tau_D \gg \tau_E$. Since τ_E grows only very slowly as $\lambda_F \rightarrow 0$, one may think of a suitable simultaneous shrinking of the width of the leads. This is the regime in which universality due to chaos is expected (for studies considering the situation when $\tau_E \gtrsim \tau_D$, see [15] and references therein), and RMT predicts that the transmission eigenvalues are distributed in the interval $[1 - 4\xi, 1]$ with average density given by [2, 16]

$$\rho(T) = \frac{N}{2\pi T} \sqrt{\frac{4\xi}{1-T} - 1}. \quad (1)$$

Here $N = N_1 + N_2$ is the total number of channels and the variable ξ is defined as

$$\xi = \frac{N_1 N_2}{N^2}. \quad (2)$$

This result is valid to leading order in N^{-1} , and is the same for all universality classes. The presence or absence of time-reversal symmetry is only felt in higher-order terms, sometimes called ‘weak-localization’ corrections.

The function $\rho(T)$ can be characterized by its moments,

$$M_m = \int \rho(T) T^m dT = \langle \text{Tr}[(tt^\dagger)^m] \rangle, \quad (3)$$

where the brackets denote an average over the corresponding random matrix ensemble. The first two moments are related to the conductance ($\propto M_1$) and to the shot noise ($\propto M_1 - M_2$). For general m , the RMT moments were calculated explicitly [17],

$$M_m = N\xi \sum_{p=0}^{m-1} \binom{m-1}{p} (-1)^p c_p \xi^p + O(1), \quad N \rightarrow \infty, \quad (4)$$

where $c_p = \binom{2p}{p}/(p+1)$ are the Catalan numbers. Alternatively, they can be encoded in the generating function [18]

$$G(s) = \sum_{m=1}^{\infty} M_m s^{m-1} = \frac{N}{2s} \left(\sqrt{1 + \frac{4\xi s}{1-s}} - 1 \right). \quad (5)$$

This is the function we shall obtain semiclassically.

3. The semiclassical approximation

A semiclassical approximation to the t_{io} element of the transmission matrix is available from the corresponding theory for the Green's function [3]. It is given as a sum over all trajectories connecting incoming channel i to outgoing channel o ,

$$t_{io} = \sum_{\gamma:i \rightarrow o} A_\gamma e^{iS_\gamma/\hbar}, \quad (6)$$

where as usual S_γ is the action of trajectory γ and A_γ is related to its stability. The semiclassical expression for the moments contains $2m$ sums over classical trajectories,

$$M_m^{\text{sc}} = \sum_{i,o} \sum_{\gamma,\sigma} \prod_{j=1}^m A_{\gamma_j} A_{\sigma_j}^* \langle e^{i(S_\gamma - S_\sigma)/\hbar} \rangle. \quad (7)$$

Here $i = \{i_1, \dots, i_m\}$ and $o = \{o_1, \dots, o_m\}$ are sets of m incoming and outgoing channels, respectively.

We are denoting by γ and σ two sets of m scattering trajectories: γ_j goes from i_j to o_j while σ_j goes from i_{j+1} to o_j ($i_{m+1} \equiv i_1$). The quantities $S_\gamma = \sum_j S_{\gamma_j}$ and $S_\sigma = \sum_j S_{\sigma_j}$ are the total actions of these sets. The average in (7) is taken around a classically small energy window, small enough to keep the classical dynamics and the amplitudes A_γ essentially unchanged. The phase factor on the other hand is rapidly oscillating as $\hbar \rightarrow 0$, and this selects from the sum only correlated trajectories, with total action difference of order \hbar . We restrict ourselves to the leading order in N^{-1} .

In what follows we identify the classical trajectories possessing the required correlations and therefore contributing to (7). These are sets of trajectories involving encounters, examples of which are shown in figure 1. A pair (γ, σ) will contribute to (7) only if there are places where γ -trajectories come very close to each other, forming an ‘encounter’, and the corresponding σ -trajectories are obtained by a process of ‘reconnection’ at the encounters, such that σ_j initially runs closely to γ_{j+1} and ends up running closely to γ_j . An encounter involving ℓ trajectories is called an ℓ -encounter. In between encounters the trajectories follow arcs, along which the two sets are practically indistinguishable. The duration of a typical encounter is of the order of the Ehrenfest time τ_E , much smaller than the typical duration of an arc which

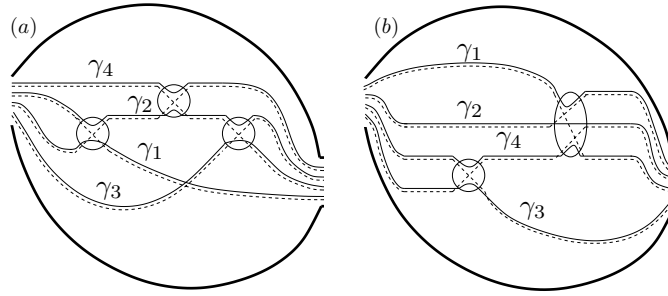


Figure 1. Schematic examples of correlated sets of classical trajectories contributing to M_4^{sc} . Each trajectory γ_j goes from incoming channel i_j to outgoing channel o_j , and is represented by a solid line. Trajectories σ_j , which go from i_{j+1} to o_j , are in dashed lines. The circles mark the encounters, where trajectories switch partners (see text).

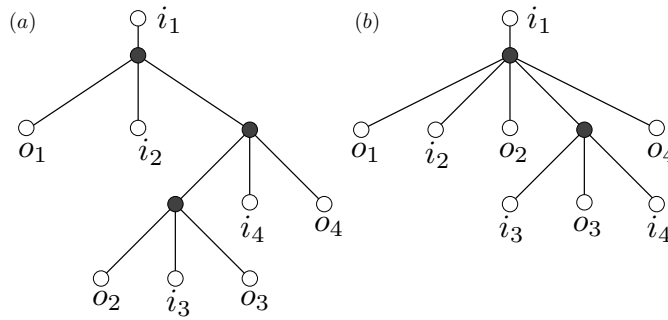


Figure 2. The trees that correspond to figure 1. The edges are the common arcs, the empty circles are the lead channels and the shaded circles (nodes) are the encounters. The edge emerging from i_1 is the root, and the channels are leaves. Note that the leaves are ordered $i_1, o_1, i_2, \dots, o_m$, starting with the root and going anti-clockwise.

is proportional to the mean dwell time τ_D . The action difference between the two sets of trajectories comes almost entirely from the vicinity of the encounters, and thus becomes small in the semiclassical limit. This theory has been discussed in several previous semiclassical calculations [4, 5, 7–11].

To perform the calculation we must construct all possible sets γ , and to this end we represent each set by a diagram containing its ‘backbone’ morphology of arcs and encounters. The complicated arcs of the actual trajectories are represented by straight edges; the encounters are represented by vertices of even degree (ℓ -encounter has degree 2ℓ) and the lead channels are represented by vertices of degree 1. The former vertices will be called *nodes* and denoted by shaded circles, see figure 2. The vertices of degree 1 will be called *leaves* and denoted by empty circles. We will see that our diagrams happen to be of a special kind, namely rooted planar trees.

With each of these diagrams we associate a vector $\mathbf{v} = (v_2, v_3, \dots)$, where v_ℓ is the number of ℓ -nodes (or ℓ -encounters). For example, one of the graphs in figure 2 has characteristic $\mathbf{v} = (3)$, and the other has characteristic $\mathbf{v} = (1, 1)$. If a diagram has characteristic \mathbf{v} , it contains $V(\mathbf{v}) = \sum_\ell v_\ell$ nodes, while the number of edges is $L(\mathbf{v}) = m + \sum_\ell \ell v_\ell$. Simple rules have been established to ‘read off’ the contribution of a given pair (γ, σ) to M_m^{sc} , starting

with the work of Richter and Sieber on weak-localization [4] which considered the simplest diagrams and derived an important sum rule. This was later generalized by Haake *et al* in order to treat all possible diagrams (see [7, 10]). Their derivation involves setting local coordinates at the encounters using Poincaré sections and invoking ergodicity to write down a probability density for encounters leading to an action difference ΔS . They then integrate over ΔS and the possible duration of the arcs and apply the sum rule. We do not repeat this procedure, which has been reviewed in detail in [5]. The final result is that *each arc contributes* $1/N$, while *each encounter contributes* $-N$. In the following sections we will use these rules together with an enumeration of the contributing diagrams to recover the random matrix prediction (4) semiclassically.

4. No coinciding channels

Let us initially assume that all channels are distinct, and do some simple power-counting with the channel number. There are a total of $\sum_{i,o} = N_1^m N_2^m$ possibilities for distributing the incoming and outgoing channels. Suppose that we have found a pair (γ, σ) represented by a graph with characteristic \mathbf{v} . The edges produce a factor of $1/N^{L(\mathbf{v})}$, while the nodes produce $(-N)^{V(\mathbf{v})}$. We thus have $N_1^m N_2^m / N^{L(\mathbf{v}) - V(\mathbf{v})}$. We want our result to be of leading order, so we must maximize $\tilde{V}(\mathbf{v}) - L(\mathbf{v})$, where $\tilde{V} = V + 2m$ is the total number of vertices (including encounters and channels). The quantity $\tilde{V}(\mathbf{v}) - L(\mathbf{v})$ is the negative of the Euler characteristic of the diagram, and it is well known that its maximal value is 1. Our moments therefore scale linearly with the number of channels, in agreement with (4). Moreover, it is also known that $\tilde{V} - L = 1$ if and only if the diagram is a tree.

As the root of the tree we choose the edge containing i_1 . The defining feature of the diagram is the existence of a traversal $i_1 \rightarrow o_1 \rightarrow i_2 \rightarrow \dots \rightarrow o_m \rightarrow i_1$, such that each edge is traversed exactly twice: once in each direction. This implies that all leaves below any given node ('below' in the sense of the natural ordering with the root being on the top) are consecutive with respect to the above traversal. Inductively, one can conclude that the branches of the diagram can be arranged in such a way that the leaves are ordered $i_1, o_1, i_2, \dots, o_m$, starting with the root and going anti-clockwise. Conversely, any tree with v_j nodes of degree $2j$ and the leaves marked $i_1, o_1, i_2, \dots, o_m$ anti-clockwise represents a diagram. A trajectory γ_1 , for example, can be read off a tree by going from i_1 to o_1 along the shortest path. Thus we have established that the diagrams contributing to the leading order are in a one-to-one correspondence with *planar* rooted trees. The term 'planar' refers to the fact that the tree is defined up to an orientation-preserving homeomorphism of the plane onto itself, i.e. swapping the branches (generally) changes the tree.

The total contribution of such a tree to M_m^{sc} is simply $(-1)^{V(\mathbf{v})} N \xi^m$. A tree with characteristic \mathbf{v} has $L(\mathbf{v}) - V(\mathbf{v}) + 1$ leaves so we denote by $d(\mathbf{v}) = (L(\mathbf{v}) - V(\mathbf{v}) + 1)/2$ the number of incoming/outgoing channels associated with trees of characteristic \mathbf{v} . If $\mathcal{N}(\mathbf{v})$ denotes the number of trees characterized by \mathbf{v} , then their combined contribution is $N \xi^m C_m$ with

$$C_m = \sum_{\mathbf{v}:d(\mathbf{v})=m} \mathcal{N}(\mathbf{v})(-1)^{V(\mathbf{v})}. \tag{8}$$

The function $\mathcal{N}(\mathbf{v})$ was studied by Tutte [19], who found an explicit formula for it,

$$\mathcal{N}(\mathbf{v}) = \frac{(\tilde{V} - 2)!}{(2m - 1)! \prod_j v_j!}. \tag{9}$$

However, for the sake of introducing the machinery needed in the following section, we take a different route and compute the above sum by making use of generating functions. The main idea is to note that if

$$f(x_2, x_3, \dots) = \sum_{\mathbf{v}} \mathcal{N}(\mathbf{v}) x_2^{v_2} x_3^{v_3} \dots \quad (10)$$

is the generating function of $\mathcal{N}(\mathbf{v})$ then $g(r)$, obtained by setting $x_{n+1} = -r^n$, is the generating function of the numbers C_m ,

$$g(r) = f(-r, -r^2, \dots) = \sum_{\mathbf{v}} \mathcal{N}(\mathbf{v}) (-1)^{V(\mathbf{v})} r^{d(\mathbf{v})} = \sum_{m=1}^{\infty} C_m r^{m-1}. \quad (11)$$

A tree characterized by \mathbf{v} contains subtrees emerging from the top $(n + 1)$ -node, which may be characterized by their own node vectors $\mathbf{v}_1, \dots, \mathbf{v}_{2n+1}$, numbering left to right. One can therefore count the number of trees characterized by \mathbf{v} by counting all possible subtrees. This implies a recursion relation for $\mathcal{N}(\mathbf{v})$ (see the appendix for details),

$$\mathcal{N}(\mathbf{v}) = \sum_{n \geq 1} \sum_{\mathbf{v}_1 \dots \mathbf{v}_{2n+1}} \prod_{j=1}^{2n+1} \mathcal{N}(\mathbf{v}_j) \delta_{\mathbf{w}, \mathbf{v} - \mathbf{e}_{n+1}}, \quad (12)$$

where $\mathbf{w} = \sum_j \mathbf{v}_j$ and \mathbf{e}_n has 1 in the n th entry and zero everywhere else. Substituting the recursion relation into equation (10) we see that f satisfies $f = 1 + x_2 f^3 + x_3 f^5 + \dots$. Correspondingly $g = 1 - r g^3 - r^2 g^5 - \dots$. Summing the geometric series we arrive at $g = 1 - r g^2$, and thus

$$g(r) = \frac{-1 + \sqrt{1 + 4r}}{2r}. \quad (13)$$

When compared with the generating function for the Catalan numbers c_m this gives

$$C_m = (-1)^{m-1} c_{m-1}, \quad (14)$$

in agreement with equation (4).

5. Coinciding channels

The previous calculations assumed all channels to be different. If it happens that $i_j = i_{j+1}$, then γ_j and γ_{j+1} enter the cavity from the same channel. It is useful to view the corresponding diagram as arising from a more general one (with $i_j \neq i_{j+1}$), in the limit when a particular encounter happens closer and closer to one of the leads. After taking this formal limit, all trajectories previously involved in the encounter now enter from the same channel, and the encounter has disappeared. This is illustrated in figure 3 for a simple example with $m = 3$. We are actually neglecting any spatial dimension the encounter may have and treating it as point-like. This is justified insofar as we consider $\tau_E \ll \tau_D$, since the length and width of encounters are typically proportional to the Ehrenfest time.

As a side note, let us mention that this subject generated some controversy when shot noise was considered in [9, 10]. Reference [10] was only interested in the $\tau_E \ll \tau_D$ regime, and considered a ‘diagonal approximation’ to the case of equal channels which is equivalent to what we discussed above. This was criticized by the authors of [9], who argued that such an approximation overlooked important corrections and would lead to the breakup of unitarity as soon as the Ehrenfest time was not negligible (this subject was also discussed in [20] from the point of view of coherent back-scattering). However, a careful analysis [21] of the stationary phase approximation shows that the corrections mentioned in [9] do indeed amount to zero

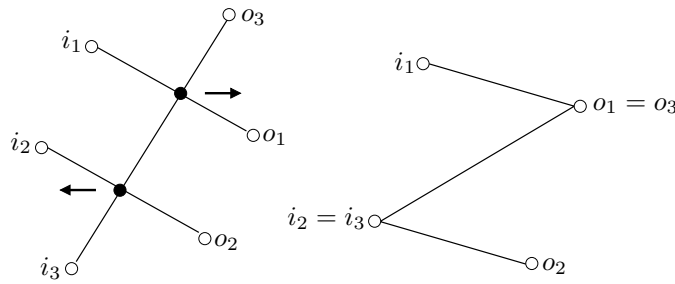


Figure 3. The diagram on the right, which has coinciding channels, is seen as a limiting case of the more general diagram on the left. The encounters are continuously brought up to the leads, and eventually disappear as all involved trajectories enter (or leave) from the same channel.

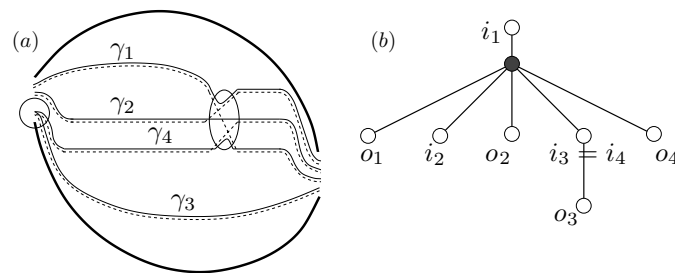


Figure 4. Left: schematic of trajectories contributing to M_4^{sc} when $i_3 = i_4$. The crossing ‘touches’ the incoming lead. Right: the corresponding tree. Compared to the tree in figure 2(b) the number of segments is reduced by two, and the number of crossings is reduced by one.

when $\tau_E \ll \tau_D$, as long as the γ -trajectories are uncorrelated and uniformly distributed in the phase space of the leads. This is consistent with the random matrix theory philosophy of assuming complete randomness.

In the situation we have described, we say that the node ‘touches’ the lead, which may be incoming or outgoing. In any case, it no longer gives the usual $-N$ contribution. We now have to count in how many ways a given one of our trees can have nodes touching leads. Consider for example the tree in figure 2(a). The lower node has two edges leading to outgoing leaves. This node could touch the outgoing lead, and hence these edges would actually vanish. The top node could touch the incoming lead, while the middle node cannot be made to touch any of the leads. In figure 4 we show the schematics and the corresponding tree of a contribution similar to figure 1(b) but with $i_3 = i_4$.

When an $(n + 1)$ -node touches an incoming lead, the number of edges is reduced by $n + 1$. The number of nodes is reduced by 1, so the contribution gets multiplied by $-N^n$. Because the number of channels involved in the sum is also reduced, there is a factor of N_1^{-n} . If we define $z_1 = N/N_1$, making an $(n + 1)$ -node touch the incoming lead produces a factor $-z_1^n$ multiplying the contribution of the tree. For a given tree T , denote by $q_{1,n}(T)$ the number of $(n + 1)$ -nodes that can be made to touch the incoming lead. There are $\binom{q_{1,n}}{k}$ ways to have k out of the $q_{1,n}$ such nodes actually touch the lead. Therefore, the basic contribution must be multiplied by

$$\sum_{k=0}^{q_{1,n}} (-z_1^n)^k \binom{q_{1,n}}{k} = (1 - z_1^n)^{q_{1,n}}. \tag{15}$$

It is easy to see that each and every diagram with coinciding channels can be derived from one and only one ‘parent’ diagram, which does not have any coinciding channels. The conclusion is that we may consider only these ‘parent’ diagrams, provided we multiply each one of them by $(1 - z_1^n)^{q_{1,n}} (1 - z_2^n)^{q_{2,n}}$, where the subscript 2 refers to the outgoing lead. This accounts for all possible contributions in which channels coincide.

The above arguments amount to saying that, similarly to (8), the complete semiclassical moments are given by

$$M_m^{\text{sc}}(\xi) = N \xi^m \sum_{\mathbf{v}:d(\mathbf{v})=m} (-1)^{V(\mathbf{v})} P(z_1, z_2; \mathbf{v}), \quad (16)$$

where the sum is over all characteristic vectors \mathbf{v} . Instead of including only the number $\mathcal{N}(\mathbf{v})$, as in (8), we must instead use

$$P(z_1, z_2; \mathbf{v}) = \sum_{T \in \mathcal{T}_{\mathbf{v}}, n \geq 1} \prod (1 - z_1^n)^{q_{1,n}(T)} (1 - z_2^n)^{q_{2,n}(T)}, \quad (17)$$

where the sum is over $\mathcal{T}_{\mathbf{v}}$ the set of all trees characterized by \mathbf{v} . Note that $z_1 z_2 = z_1 + z_2 = \xi^{-1}$. Now we define the generating function of P ,

$$F(z_1, z_2; x_2, x_3, \dots) = \sum_{\mathbf{v}} P(z_1, z_2; \mathbf{v}) x_2^{v_2} x_3^{v_3} \dots, \quad (18)$$

and, by defining $G^{\text{sc}}(r) = N \xi F(z_1, z_2; -r, -r^2, \dots)$, we obtain the analogue of (11) as

$$G^{\text{sc}}(r) = N \xi \sum_{m=1}^{\infty} \frac{M_m^{\text{sc}}(\xi)}{N \xi^m} r^{m-1} = \sum_{m=1}^{\infty} M_m^{\text{sc}}(\xi) \left(\frac{r}{\xi}\right)^{m-1}. \quad (19)$$

Unfortunately, it is not straightforward to write a recursion for P . This is because, unlike any other node in the tree, the top node can be made to touch *both* leads (although not at the same time). To circumvent this problem, we define an auxiliary function,

$$\tilde{P}(z_1, z_2; \mathbf{v}) = \sum_{T \in \mathcal{T}_{\mathbf{v}}, n \geq 1} \prod (1 - z_1^n)^{q'_{1,n}(T)} (1 - z_2^n)^{q_{2,n}(T)}, \quad (20)$$

where $q'_{1,n}$ is defined as $q_{1,n}$ but excluding the top node. For \tilde{P} there is a natural recursion relation, analogous to (12), explained in the appendix. It is given by

$$\begin{aligned} \tilde{P}(z_1, z_2; \mathbf{v}) &= \sum_{n \geq 1} \sum_{\mathbf{v}_1 \dots \mathbf{v}_{2n+1}} \tilde{P}(z_1, z_2; \mathbf{v}_1) \\ &\times \prod_{j=1}^n \tilde{P}(z_2, z_1; \mathbf{v}_{2j}) \tilde{P}(z_1, z_2; \mathbf{v}_{2j+1}) (1 - z_2^n \delta_{\mathbf{u}, \mathbf{0}}) \delta_{\mathbf{w}, \mathbf{v} - \mathbf{e}_{n+1}}, \end{aligned} \quad (21)$$

where again we use $\mathbf{w} = \sum_{j=0}^{2n+1} \mathbf{v}_j$ and $\mathbf{u} = \sum_{j=0}^n \mathbf{v}_{2j+1}$. The sum is over the valency of the top node and the characteristic vectors of the $2n + 1$ subtrees that emanate from it. The factor $z_2^n \delta_{\mathbf{u}, \mathbf{0}}$ includes the contribution due to the top node touching the outgoing lead which is only possible when all odd \mathbf{v}_j 's vanish. The function \tilde{P} is useful because it is related to P according to

$$\begin{aligned} P(z_1, z_2; \mathbf{v}) &= \sum_{n \geq 1} \sum_{\mathbf{v}_1 \dots \mathbf{v}_{2n+1}} \tilde{P}(z_1, z_2; \mathbf{v}_1) \prod_{j=1}^n \tilde{P}(z_2, z_1; \mathbf{v}_{2j}) \\ &\times \tilde{P}(z_1, z_2; \mathbf{v}_{2j+1}) (1 - z_1^n \delta_{\mathbf{w}, \mathbf{u}} - z_2^n \delta_{\mathbf{u}, \mathbf{0}}) \delta_{\mathbf{w}, \mathbf{v} - \mathbf{e}_{n+1}}, \end{aligned} \quad (22)$$

which now includes the contribution due to the top node touching the incoming lead when all the even \mathbf{v}_j 's vanish. The details are also left to the appendix.

We now denote by $f(z_1, z_2; \mathbf{x})$ the generating function of \tilde{P} . The recursion relation (21) implies

$$f(z_1, z_2; \mathbf{x}) = 1 + \sum_{n \geq 1} x_{n+1} (f^{n+1}(z_1, z_2; \mathbf{x}) - z_2^n) f^n(z_2, z_1; \mathbf{x}). \quad (23)$$

We again identify $x_{n+1} = -r^n$ and write $g(z_1, z_2; r) = f(z_1, z_2; -r, -r^2, \dots)$. Making use of the geometric series, we can reduce (23) to

$$g(z_1, z_2; r) = 1 + r(z_2 - 1)h(z_1, z_2; r), \quad (24)$$

where we have defined a function which is symmetric with respect to the variables z_1, z_2 , namely $h(z_1, z_2; r) = g(z_1, z_2; r)g(z_2, z_1; r)$. Substituting (24) back into h leads to the algebraic equation

$$\xi h = \xi(1 - rh)^2 + rh, \quad (25)$$

which can be solved to give

$$h = \frac{\xi + 2\xi r - r - \sqrt{(\xi - r)(4\xi r + \xi - r)}}{2\xi r^2}. \quad (26)$$

Having this solution we can compute $g(z_1, z_2; r)$. Because of (22), the function $f(z_1, z_2; \mathbf{x})$ is related to $F(z_1, z_2; \mathbf{x})$ simply by $F = f - \sum_{n \geq 1} x_{n+1} z_1^n f^{n+1}$. This implies that

$$G^{\text{sc}}(r) = \frac{N\xi g(z_1, z_2; r)}{1 - rz_1 g(z_1, z_2; r)}. \quad (27)$$

Let us multiply and divide the above expression by $(1 - rz_2 g(z_2, z_1; r))$. We may then use that

$$(1 - rz_1 g(z_1, z_2; r))(1 - rz_2 g(z_2, z_1; r)) = \frac{\xi - r}{\xi}, \quad (28)$$

by virtue of (24) and the definition of $z_{1,2}$. On the other hand, using (24) again

$$g(z_1, z_2; r)(1 - rz_2 g(z_2, z_1; r)) = 1 - rh. \quad (29)$$

Finally, taking the explicit formula (26) into account and writing $s = r/\xi$ leads to

$$\sum_{m=1}^{\infty} M_m^{\text{sc}}(\xi) s^{m-1} = \frac{N}{2s} \left(\sqrt{1 + \frac{4\xi s}{1-s}} - 1 \right), \quad (30)$$

which is identical to (5). Therefore, all semiclassical moments are indeed equal to the corresponding random matrix theory predictions. From the semiclassical point of view, the fact that the leading order result is the same with or without time-reversal symmetry stems from the fact that, being trees, the contributing diagrams contain no loops (in contrast to Richter–Sieber pairs [4], for example).

Obtaining higher-order terms in N^{-1} , which are necessary to describe experiments in which a relatively small number of channels are involved, would require the incorporation of more general sets of trajectories, for which the corresponding diagrams are no longer trees. Computing the full perturbative series seems to be a very demanding task, especially for systems with time-reversal symmetry. We should mention that some exact RMT results (valid for arbitrary channel numbers) have appeared recently [22, 23]. In particular, for broken time-reversal symmetry the average values of $\text{Tr } T^m$, $(\text{Tr } T^m)^2$ and $(\text{Tr } T)^m$, where $T = tt^\dagger$, were obtained for general m by one of the present authors [24].

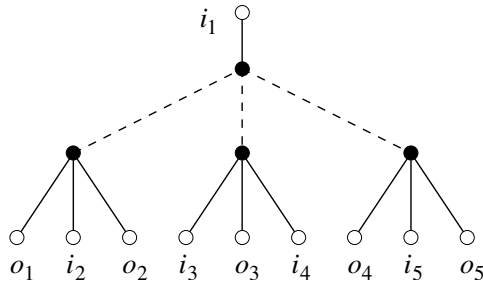


Figure A1. A tree with characteristic $\mathbf{v} = (4)$ separates at the top node into three subtrees characterized by $\mathbf{v}_1 = \mathbf{v}_2 = \mathbf{v}_3 = (1)$.

Acknowledgments

We have profited from interesting discussions with R S Whitney. GB and JMH were supported by NFS grant DMS-0604859. MN was supported by EPSRC.

Appendix A. Tree recursion relations

Let T be a tree and $\mathcal{T}_{\mathbf{v}}$ the set of trees with characteristic \mathbf{v} . We first establish the recurrence relation (12) for $\mathcal{N}(\mathbf{v}) = |\mathcal{T}_{\mathbf{v}}|$, the number of trees characterized by the node vector \mathbf{v} . To derive the relation we break the tree at the top $(n + 1)$ -node adjacent to the root. The top node has degree $2(n + 1)$ and splitting the tree T at this point the node becomes the root of $2n + 1$ subtrees T_1, \dots, T_{2n+1} , characterized by vectors $\mathbf{v}_1, \dots, \mathbf{v}_{2n+1}$. Clearly $\mathbf{v} = \sum_{j=1}^{2n+1} \mathbf{v}_j + \mathbf{e}_{n+1}$ where \mathbf{e}_n has 1 in its n th entry and zero elsewhere, representing the top node that was removed. Figure A1 shows a tree with characteristic (4). This tree splits at the top node, degree four ($n = 1$), into three subtrees each characterized by (1). In general the number of trees with top node degree $2(n + 1)$ is given by the number of combinations of subtrees, $\prod_{j=1}^{2n+1} \mathcal{N}(\mathbf{v}_j)$ where $\mathbf{w} = \sum_{j=1}^{2n+1} \mathbf{v}_j = \mathbf{v} - \mathbf{e}_{n+1}$. Summing over all allowed valencies of the top node establishes the recursion relation,

$$\mathcal{N}(\mathbf{v}) = \sum_{n \geq 1} \sum_{\mathbf{v}_1 \cdots \mathbf{v}_{2n+1}} \prod_{j=1}^{2n+1} \mathcal{N}(\mathbf{v}_j) \delta_{\mathbf{w}, \mathbf{v} - \mathbf{e}_{n+1}}. \tag{A.1}$$

The recursion relation (21) for \tilde{P} can be generated in a similar manner. To recap,

$$\tilde{P}(z_1, z_2; \mathbf{v}) = \sum_{T \in \mathcal{T}_{\mathbf{v}}} \prod_{m \geq 1} (1 - z_1^m)^{q'_{1,m}(T)} (1 - z_2^m)^{q_{2,m}(T)}, \tag{A.2}$$

where $q_{2,m}(T)$ is the number of ways an $(m + 1)$ -node can touch the outgoing lead and $q'_{1,m}(T)$ the number of $(m + 1)$ -nodes—excluding the top node adjacent to the root—that can touch the incoming lead. For our trees the root corresponds to the incoming lead and our definition of \tilde{P} excludes the possibility of touching the root.

To establish the recursion relation we again consider breaking the tree into subtrees T_1, \dots, T_{2n+1} at the top $(n + 1)$ -node, numbering left to right. The number of ways an $(m + 1)$ -node of the tree can touch the incoming lead is

$$q'_{1,m}(T) = q'_{1,m}(T_1) + \sum_{j=1}^n (q_{2,m}(T_{2j}) + q'_{1,m}(T_{2j+1})). \tag{A.3}$$

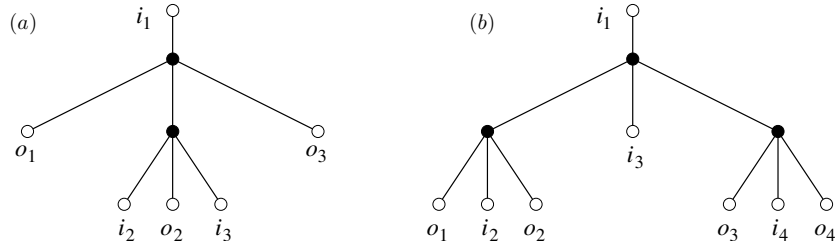


Figure A2. (a) A tree with characteristic $\mathbf{v} = (2)$ where the top node can be made to touch the outgoing lead. (b) A tree with characteristic $\mathbf{v} = (3)$ where the top node can be made to touch the incoming lead.

This includes a change in the ordering of the leaves on the subtrees with even index. On subtrees with odd index the first (left most) leaf must be an outgoing lead, labelled o , while the first lead of an even numbered subtree is labelled with the incoming lead i , see for example figure A1.

To find the number of ways an $(m + 1)$ -node can touch the outgoing lead, similarly one sums the $q_{2,m}$ of the odd subtrees and adds the $q'_{1,m}$ of the even subtrees where the o and i leaf labels must be exchanged. In addition if $m = n$ the top node can contribute. The top node may be made to touch the outgoing lead if all the odd subtrees have characteristic $\mathbf{0}$, i.e. every odd edge ends in a leaf. Figure A2(a) shows a tree where the top node can touch the outgoing lead. Therefore,

$$q_{2,m}(T) = q_{2,m}(T_1) + \sum_{j=1}^n (q'_{1,m}(T_{2j}) + q_{2,m}(T_{2j+1})) + \delta_{\mathbf{u},\mathbf{0}}\delta_{m,n}, \tag{A.4}$$

where $\mathbf{u} = \sum_{j=0}^n \mathbf{v}_{2j+1}$. Consequently $\tilde{P}(z_1, z_2; \mathbf{v})$ is expressed in terms of functions $\tilde{P}(\cdot, \cdot; \mathbf{v}_j)$ generated by the subtrees,

$$\begin{aligned} \tilde{P}(z_1, z_2; \mathbf{v}) &= \sum_{n \geq 1} \sum_{\mathbf{v}_1 \cdots \mathbf{v}_{2n+1}} \tilde{P}(z_1, z_2; \mathbf{v}_1) \\ &\times \prod_{j=1}^n \tilde{P}(z_2, z_1; \mathbf{v}_{2j}) \tilde{P}(z_1, z_2; \mathbf{v}_{2j+1}) (1 - z_2^n \delta_{\mathbf{u},\mathbf{0}}) \delta_{\mathbf{w}, \mathbf{v} - \mathbf{e}_{n+1}}. \end{aligned} \tag{A.5}$$

From \tilde{P} we recover P by calculating the contribution generated when the top node touches the incoming lead independently. Recall the definition of P ,

$$P(z_1, z_2; \mathbf{v}) = \sum_{T \in \mathcal{T}_{\mathbf{v}}} \prod_{m \geq 1} (1 - z_1^m)^{q_{1,m}(T)} (1 - z_2^m)^{q_{2,m}(T)}. \tag{A.6}$$

Comparing this with the definition of \tilde{P} (A.2), we see that terms in the sum are identical except when the top $(n+1)$ -node of T can touch the incoming lead, in which case $q_{1,n}(T) = q'_{1,n}(T)+1$. If we let $\mathcal{R}_{\mathbf{v}} \subset \mathcal{T}_{\mathbf{v}}$ denote the set of trees that can touch the root the definition of P can be rewritten using \tilde{P} :

$$P(z_1, z_2; \mathbf{v}) = \tilde{P}(z_1, z_2; \mathbf{v}) - \sum_{T \in \mathcal{R}_{\mathbf{v}}} z_1^n \prod_{m \geq 1} (1 - z_1^m)^{q'_{1,m}(T)} (1 - z_2^m)^{q_{2,m}(T)}, \tag{A.7}$$

where n is determined by the degree of the node adjacent to the root. A tree is in $\mathcal{R}_{\mathbf{v}}$ if, counting left to right, the even branches of the top node all end in leaves, $\mathbf{v}_{2j} = \mathbf{0}$ for $j \in \{1, \dots, n\}$ or

equivalently $\mathbf{w} = \mathbf{u}$. Figure A2(b) shows a tree in \mathcal{R}_v . In equation (A.7) the product inside the sum over \mathcal{R}_v is the same as that appearing in the definition of \tilde{P} and we can again break the trees in \mathcal{R}_v at the top node to write the contribution in terms of subtrees. Combining this with the recursion relation (A.5) for \tilde{P} , we obtain the following formula for P :

$$P(z_1, z_2; \mathbf{v}) = \sum_{n \geq 1} \sum_{\mathbf{v}_1 \cdots \mathbf{v}_{2n+1}} \tilde{P}(z_1, z_2; \mathbf{v}_1) \prod_{j=1}^n \tilde{P}(z_2, z_1; \mathbf{v}_{2j}) \\ \times \tilde{P}(z_1, z_2; \mathbf{v}_{2j+1}) (1 - z_1^n \delta_{\mathbf{w}, \mathbf{u}} - z_2^n \delta_{\mathbf{u}, \mathbf{0}}) \delta_{\mathbf{w}, \mathbf{v} - \mathbf{e}_{n+1}} \quad (\text{A.8})$$

References

- [1] Ferry D K and Goodnick S M 1997 *Transport in Nanostructures* (Cambridge: Cambridge University Press)
- [2] Baranger H U and Mello P A 1994 *Phys. Rev. Lett.* **73** 142
Jalabert R A, Pichard J-L and Beenakker C W J 1994 *Europhys. Lett.* **27** 255
Beenakker C W J 1997 *Rev. Mod. Phys.* **69** 731
- [3] Jalabert R A, Baranger H U and Stone A D 1990 *Phys. Rev. Lett.* **65** 2442
Baranger H U, Jalabert R A and Stone A D 1993 *Chaos* **3** 665
- [4] Richter K and Sieber M 2002 *Phys. Rev. Lett.* **89** 206801
- [5] Müller S, Heusler S, Braun P and Haake F 2007 *New J. Phys.* **9** 12
- [6] Berry M V 1985 *Proc. R. Soc. Lond. A* **400** 229
Argaman N *et al* 1993 *Phys. Rev. Lett.* **71** 4326
Sieber M 2002 *J. Phys. A: Math. Gen.* **35** L613
Muller S *et al* 2004 *Phys. Rev. Lett.* **93** 014103
Heusler S *et al* 2007 *Phys. Rev. Lett.* **98** 044103
- [7] Adagideli I 2003 *Phys. Rev. B* **68** 233308
Rahav S and Brouwer P W 2005 *Phys. Rev. Lett.* **95** 056806
Heusler S, Müller S, Braun P and Haake F 2006 *Phys. Rev. Lett.* **96** 066804
- [8] Schanz H, Puhlmann M and Geisel T 2003 *Phys. Rev. Lett.* **91** 134101
- [9] Whitney R S and Jacquod Ph 2006 *Phys. Rev. Lett.* **96** 206804
- [10] Braun P, Heusler S, Müller S and Haake F 2006 *J. Phys. A: Math. Gen.* **39** L159
- [11] Kuipers J and Sieber M 2007 *Nonlinearity* **20** 909
- [12] Nazarov Yu V (ed) 2003 *Quantum Noise in Mesoscopic Physics* (Dordrecht: Kluwer)
- [13] Blanter Ya M, Schomerus H and Beenakker C W J 2001 *Physica E (Amsterdam)* **11** 1
Bulashenko O M 2005 *J. Stat. Mech.* **P08013**
- [14] Reulet B, Senzier J and Prober D E 2003 *Phys. Rev. Lett.* **91** 196601
Bomze Yu *et al* 2005 *Phys. Rev. Lett.* **95** 176601
Gustavsson S *et al* 2006 *Phys. Rev. Lett.* **96** 076605
- [15] Schomerus H and Jacquod Ph 2005 *J. Phys. A: Math. Gen.* **38** 10663
Jacquod Ph and Whitney R S 2006 *Phys. Rev. B* **73** 195115
Brouwer P W and Rahav S 2006 *Phys. Rev. B* **74** 075322
- [16] Nazarov Y 1995 *Quantum Dynamics of Submicron Structures* ed H A Cerdeira, B Kramer and G Schön (Dordrecht: Kluwer)
- [17] Novaes M 2007 *Phys. Rev. B* **75** 073304
- [18] Brouwer P W and Beenakker C W J 1996 *J. Math. Phys.* **37** 4904
- [19] Tutte W T 1964 *Am. Math. Mon.* **71** 272
- [20] Rahav S and Brouwer P W 2006 *Phys. Rev. Lett.* **96** 196804
- [21] Whitney R S unpublished
- [22] Sommers H-J, Wicczorek W and Savin D V 2007 *Acta Phys. Pol. A* **112** 691
Savin D V, Sommers H-J and Wicczorek W 2008 *Phys. Rev. B* **77** 125332
- [23] Araújo J E F and Macêdo A M S 1998 *Phys. Rev. B* **58** R13379
Vivo P and Vivo E 2008 *J. Phys. A: Math. Theor.* **41** 122004
- [24] Novaes M 2008 *Phys. Rev. B* **78** 035337